DMD Fast Forward. Published on November 8, 2018 as DOI: 10.1124/dmd.118.083691
This article has not been copyedited and formatted. The final version may differ from this version.

Berberine Directly Impacts the Gut Microbiota to Promote Intestinal Farnesoid X Receptor Activation

Yuan Tian, Jingwei Cai, Wei Gui, Robert G. Nichols, Imhoi Koo, Jingtao Zhang, Mallappa Anitha, Andrew D. Patterson

Department of Veterinary and Biomedical Sciences, The Pennsylvania State University, University Park, Pennsylvania 16802, United States (Y.T., J.C., W.G., R.G.N., I.K., J.Z., M.A., A.D.P.)

CAS Key Laboratory of Magnetic Resonance in Biological Systems, State Key Laboratory of Magnetic Resonance and Atomic and Molecular Physics, National Centre for Magnetic Resonance in Wuhan, Wuhan Institute of Physics and Mathematics, University of Chinese Academy of Sciences, Wuhan, 430071, P. R. China (Y.T.)

Running title: Berberine directly impacts the gut microbiota to promote intestinal farnesoid X receptor activation

Corresponding author: Andrew D. Patterson, Email: adp117@psu.edu, Address: 322 Life Science Bldg, University Park, PA 16802, Phone: 814-867-4565

Number of text pages: 24

Number of figures: 8

Number of references: 49

Number of words in the Abstract: 160

Number of words in the Introduction: 509

Number of words in the Discussion: 794

Non-standard abbreviations: CDCA, chenodeoxycholic acid; CFDA, carboxyfluorescein diacetate; $DiBAC_4$, bis-(1,3-dibutylbarbituric acid) trimethine oxonol; MRM, multiple reaction monitoring; NAFLD, nonalcoholic fatty liver disease; OPLS-DA, orthogonal projection to latent structure-discriminant; OUT, operation taxonomic unit; PCA, principal component analysis; PMSF, phenylmethylsulfonyl fluoride; TCDCA, taurochenodeoxycholic acid; TDCA, taurodeoxycholic acid; THDCA, taurohyodeoxycholic acid; TβMCA, tauro-β-muricholic acid; TUCA, tauroursocholanic acid; TUDCA, tauroursodeoxycholic acid; TSP, 3-(trimethylsilyl) [2,2,3,3-$^2H_4$] propionate.

Abstract

Intestinal bacteria play an important role in bile acid metabolism and in the regulation of multiple host metabolic pathways (e.g., lipid and glucose homeostasis) through modulation of intestinal farnesoid X receptor (FXR) activity. Here, we examined the effect of berberine (BBR), a natural plant alkaloid, on intestinal bacteria using in vitro and in vivo models. In vivo, the metabolomic response and changes in mouse intestinal bacterial communities treated with BBR (100 mg/kg) for 5 days were assessed using NMR- and mass spectrometry-based metabolomics coupled with multivariate data analysis. Short-term BBR exposure altered intestinal bacteria by reducing the *Clostridium* cluster XIVa and IV and their bile salt hydrolase (BSH) activity, which resulted in the accumulation of taurocholic acid (TCA). The accumulation of TCA was associated with activation of intestinal FXR, which can mediate bile acid, lipid, and glucose metabolism. In vitro, isolated mouse cecal bacteria were incubated with three doses of BBR (0.1, 1, and 10 mg/ml) for 4 h in an anaerobic chamber. NMR-based metabolomics combined with flow cytometry was used to evaluate the direct physiologic and metabolic impact of BBR on the bacteria. In vitro, BBR exposure not only altered bacterial physiology, but also changed the bacterial community composition and function, especially reducing BSH expressing bacteria like *Clostridium* spp. These data suggest that BBR directly impacts bacteria to alter bile acid metabolism and activate FXR signaling. These data provide new insights into the link between intestinal bacteria, nuclear receptor signaling, and xenobiotics.

Introduction

In addition to their well-established role in regulating the metabolism of vitamins, lipids and other hydrophobic dietary constituents, bile acids activate nuclear receptors and membrane G-protein coupled receptors to mediate lipid, glucose, and energy homeostasis (Kawamata et al., 2003; Li and Chiang, 2013). Notably, the nuclear receptor farnesoid X receptor (FXR) has gained increasing consideration as druggable receptor (Lambert et al., 2003; Duran-Sandoval et al., 2004). FXR is a ligand-activated receptor expressed in many tissues including liver, intestinal epithelium, adipose tissue, kidney, pancreas, stomach, gall bladder, and macrophage (Forman et al., 1995). FXR activation can protect against obesity, diabetes, and fatty liver disease, and can improve hyperlipidemia and hyperglycemia (Zhang et al., 2006; Ali et al., 2015; Arab et al., 2017). Recent studies also suggest that intestinal FXR agonists inhibit bacterial overgrowth and prevent bacterial translocation and epithelial deterioration (Inagaki et al., 2006). Paradoxically, similar beneficial effects towards the improvement of obesity, insulin resistance, and reduction of non-alcoholic fatty liver disease (NAFLD) are also seen with FXR antagonists (Li et al., 2013; Jiang et al., 2015a; Jiang et al., 2015b). Thus, the contextual role and tissue-dependent mechanism for the beneficial effects of FXR are important.

More recent studies indicated that intestinal bacteria play a key role in obesity and related metabolic diseases, especially by mediating bile acid biosynthesis and FXR signaling (Sayin et al., 2013; Zhang et al., 2016). Previous evidence indicated that the intestinal bacteria regulate bile acid metabolism thus resulting in FXR activation in the liver and gut (Ridlon et al., 2014). A recent study indicated a novel mechanism for the intestine-restricted FXR agonist fexaramine that can activate intestinal FXR and TGR5/GLP-1 signaling through intestinal microbiota activity to protect against obesity and related metabolic disease (Pathak et al., 2018).

Berberine (BBR), a natural plant alkaloid, is the major pharmacologic component in Chinese herbal medicine *Coptis chinensis* (Huang-Lian) (Tang et al., 2009). As a traditional Chinese medicine, BBR has been used to treat diarrhea in China (Chen et al., 2015). Accumulating evidence suggests that BBR can improve metabolic syndrome via regulation of glucose and lipid metabolism, and attenuating insulin resistance (Kong et al., 2004; Zhang et al., 2014; Xu et al., 2017). Since BBR has low bioavailability, modulation of gut bacteria might be one possible mechanism for its anti-diabetic and anti-obesity effects (Han et al., 2011; Xie et al., 2011). Recent evidence suggested the lipid-lowering effect of BBR involves modulating bile acid composition and activating intestinal FXR signaling (Guo et al., 2016; Sun et al., 2017). However, the underlying mechanisms by which BBR modulates the intestinal bacteria community leading to microbially-induced signals have not been explored.

In the present study, BBR effects on bacteria using both in vitro and in vivo models were investigated. We studied the direct effect of BBR on bacteria in vitro, so as to determine mechanisms of action in vivo. We demonstrated that BBR directly altered the gut microbiota by reducing *Clostridium* spp. and subsequently altered intestinal FXR signaling. These data provide new insights for studying the link between the intestinal bacteria, nuclear receptor signaling, and xenobiotics.

Materials and Methods

Chemicals

Berberine chloride (BBR) and brain heart infusion broth were ordered from Sigma-Aldrich (St Louis, MO). Transgenic dough was purchased from Bio-Serve (Flemington, NJ). Bile acid standards and deuterated internal standards were obtained from Sigma-Aldrich (St Louis, MO) and Cayman Chemical (Ann Arbor, MI). Four dyes including SybrGreen, propidium iodide (Pi), bis-(1,3-dibutylbarbituric acid) trimethine oxonol ($DiBAC_4$), and carboxyfluorescein diacetate (CFDA) were ordered from Invitrogen (Carlsbad, CA). Sodium 3-(trimethylsilyl) [2,2,3,3-$^2H_4$] propionate (TSP) and D_2O (99.9% in D) were bought from Cambridge Isotope Laboratories (Miami, FL). Reduced 1 × rPBS solution containing 1 g/l L-cysteine was prepared and stored anaerobically for bacterial culture.

Animals

Animal procedures were performed using protocols approved by the Pennsylvania State University Institutional Animal Care and Use Committee. Twelve male C57BL/6 wild type mice were ordered from Jackson Laboratories (Bar Harbor, MN). 5-week-old mice were trained to eat bacon-flavored dough pills for one week. Dough pills containing BBR were made using tablet molds as previously described (Zhang et al., 2015a; Zhang et al., 2016), and one pill contained 2.3 mg BBR (100 mg/kg as final dose). Mice were fed pills containing BBR or vehicle for 5 days (Fig. 1A). Mice were housed singly in an empty cage and monitored to ensure the pill was consumed. Urine and feces were collected after 0, 1, 3, and 5 days BBR treatment. Blood, liver, cecal content, and intestinal tissue samples were collected and saved at -80°C immediately after sacrifice.

Histopathology and clinical biochemistry

Embedded liver tissues in paraffin wax were stained with hematoxylin and eosin (H&E). Liver injury markers including serum alanine transaminase (ALT) and alkaline phosphatase (ALP) were performed using the VetScan Chemistry Analyzer VS2 (Abaxis Inc., Union City, CA).

Bile acid quantitation by UPLC-MS/MS

Quantitative analysis of bile acids in liver, feces, and ileum tissue was measured with an Acquity UPLC system coupled to a Waters Xevo TQS MS with an Acquity C8 BEH (2.1 × 100 mm, 1.7 μm) UPLC column (All Waters, Milford, MA). Tissues (50 mg) and feces (25 mg) were added to 1 ml methanol containing 0.5 μM deuterated internal standards followed by homogenization. Following centrifugation, analytes were detected by multiple reaction monitoring (MRM) and normalized by their respective internal deuterated standard. The results were quantified by comparing integrated peak areas against a standard curve.

Bile salt hydrolase (BSH) activity

BSH activity was measured using the published protocol (Li et al., 2013) with minor modifications. Protein was prepared from fecal samples (50 mg) with 500 μl PBS containing 1 mM phenylmethylsulfonyl fluoride (PMSF). Incubations were performed at 37°C in 3 mM sodium acetate buffer containing 0.4 mg/ml fecal protein and 5 μM TCA-d4. After 30 min incubation, an equal volume methanol was added to the reaction. Following centrifugation, the supernatant was analyzed by an Acquity UPLC system coupled with a Waters Xevo TQS MS (Waters, Milford, MA).

Tissue RNA extraction and qPCR

Liver and ileum RNA was extracted using TRIzol reagent (Invitrogen, Carlsbad, CA). cDNA was synthesized from 1 μg RNA using qScript cDNA SuperMix (Quanta Biosciences, Gaithersburg, MD). qPCR was carried out using SYBR green QPCR master mix using an ABI Prism 7900HT

DMD Fast Forward. Published on November 8, 2018 as DOI: 10.1124/dmd.118.083691
This article has not been copyedited and formatted. The final version may differ from this version.

Fast real-time PCR sequence detection system (Applied Biosystems, Waltham, MA). qPCR primers are shown in Supplementary Table S1, and data were normalized to *Actb* mRNA levels.

In vitro bacterial culture and flow cytometry

In vitro bacterial culture with BBR treatment was done using the published protocol (Maurice and Turnbaugh, 2013) with minor modifications. Briefly, cecal contents from twelve 7-week-old male C57BL/6J mice were mixed and diluted in sterile brain heart infusion broth (1:10 g/ml). After vortexing, 1.8 ml of the bacterial mixture was transferred to new tubes and divided into four groups. Three groups were treated with three doses of BBR including high (10 mg/ml), middle (1.0 mg/ml), and low (0.1 mg/ml) doses. After vortexing, incubation of the bacterial mixtures was carried out at 37°C for 4 h. After incubation, bacterial samples were stained for flow cytometry analysis or kept at -80°C for metabolite and bacteria DNA analysis (Fig. 1B). All experiments were done in a monitored anaerobic chamber.

After centrifugation of bacterial mixtures, the supernatants were washed and diluted 120 times with 1X reduced PBS. Diluted samples stained by four different dyes including SybrGreen, Pi, $DiBAC_4$, and CFDA were analyzed on a BD Accuri™ C6 flow cytometer (Franklin Lakes, NJ), and data was analyzed using FlowJo V10 software (Tree Star, Ashland, OR). The percentages of Pi, DiBAC, CFDA, low nucleic acid (LNA) and high nucleic acid (HNA) cells were normalized to SybrGreen.

Bacteria DNA extraction and qPCR

DNA was extracted from cecal contents and in vivo bacterial suspension using E.Z.N.A. ® stool DNA kit (Omega Bio-Tek Inc., Norcross, USA). qPCR was carried out with SYBR Green qPCR Master Mix on an ABI Prism 7900HT Fast Real-Time PCR sequence detection system. The primers

are shown in Supplementary Table S2, and the data were normalized to 16S ribosomal DNA sequences.

^{1}H NMR-based metabolomics experiments

Urine and feces sample preparation for NMR analysis was carried out as described (Jiang et al., 2012). Bacteria suspension samples were extracted twice with 1 ml of methanol-water mix (2/1, v/v) and followed by three consecutive freeze-thaws. After evaporation via SpeedVac, the extracts were resuspended into 600 µl PBS (0.1 M, 50% v/v D_2O, 0.005% TSP) and analyzed by a Bruker Avance III 600 MHz NMR spectrometer equipped with an inverse cryogenic probe (Bruker Biospin, Rheinstetten, Germany). A typical 1D NMR spectrum was acquired using NOESYPR1D, and principal component analysis (PCA) and orthogonal projection to latent structure-discriminant analysis (OPLS-DA) were performed with the SIMCA-P+ software (Umetrics, Sweden). The color-coded correlation coefficient plots from the OPLS-DA models were carried out with MATLAB (The Mathworks Inc., Natwick, MA).

FXR reporter assay

The agonist activities of taurine conjugated-bile acids and BBR were measured with the Human FXR Reporter Assay (INDIGO Biosciences, Inc., State College, PA). Briefly, reporter cells were incubated with taurine conjugated-bile acids or BBR for 6 h, after which luminescence was measured by plate-reader.

Statistics

Values are represented by mean ± standard deviation (SD) or median and interquartile ranges. Statistical analyses were performed using unpaired t-test analysis for the in vivo experiment and one-way ANOVA for the in vitro experiment by GraphPad Prism (v 6.0, GraphPad).

Results

BBR treatment increases taurine conjugated bile acids

No significant change in food intake, body weight, or liver histopathology were observed in the mice after BBR exposure (Supplementary Fig. S1A-B). BBR had no effect on serum ALT and ALP levels (Supplementary Fig. S1C). Previous studies indicated that BBR treatment for 2 or 8 weeks impacted bile acid biosynthesis (Guo et al., 2016; Sun et al., 2017). Analysis of bile acid composition showed that 5 days of BBR treatment significantly increased taurine-conjugated bile acid levels in feces, liver, and ileum (Fig. 2A-C). BBR treatment markedly increased TCA, tauroursodeoxycholic acid (TUDCA), taurochenodeoxycholic acid (TCDCA), and tauro-β-muricholic (TβMCA) in feces, liver, and ileum (Fig. 2A-C). No significant changes in unconjugated bile acids (Fig. 2A-C) or total bile acids (Fig. 2D) were observed after 5 days of BBR treatment. The mRNA expression of genes involved in bile acid synthesis in the liver was unchanged (Fig. 2E). These results suggest that BBR might act as an intestine-restricted FXR activator that does not alter the expression of FXR target genes involved in bile acid synthesis in the liver.

TCA activates the FXR signaling pathway

Altered bile acid signaling is associated with the FXR signaling (Lefebvre et al., 2009). BBR treatment for 5 days activated intestinal FXR target gene expression including small heterodimer partner (*Shp*) and fibroblast growth factor 15 (*Fgf15*) but remained unchanged in the liver (Fig. 3A). These data confirmed that BBR promotes intestine-restricted FXR activation. BBR treatment also increased mRNA expression of taurine transporter (*Taut*) and the relate-limiting enzyme for the conversation of cysteine to taurine (*Csd*) in the liver (Fig. 3B). The mRNA expression of bile acid conjugated enzyme (*Bacs* and *Baat*) was also significantly higher in the liver after BBR

treatment (Fig. 3B), which were consistent with the increased levels of hepatic taurine-conjugated bile acids. We also observed decreased expression of genes involved in bile acid transporters (*Ntcp* and *Oatp1*) in the liver after BBR treatment (Fig. 3B). These results are consistent with the data that suppression of these transporters by FXR involves a cascade including FXR-SHP activation (Geier et al., 2007; Dawson et al., 2009).

Previous evidence demonstrated that specific taurine-conjugated bile acids had different effects on the FXR signaling pathway (Cyphert et al., 2012). To investigate how altered taurine conjugated bile acid profiles and BBR can directly affect FXR signaling pathway, we used an FXR reporter assay to evaluate the FXR agonist activities of taurine-conjugated bile acids (TCA, TCDCA, TUDCA, and TβMCA) and BBR. In vitro, 100 μM TCA and TCDCA effectively activated FXR (increased 7.9-fold and 2.4-fold, respectively), whereas 100 μM TUDCA, TβMCA and BBR have no effect (Fig. 4). These results indicate that the activation of intestinal FXR signaling by BBR treatment is mainly due to the accumulation of TCA.

BBR treatment decreased *Clostridium* and BSH activity in mice

Earlier studies reported a significant decrease in the bacterial diversity following long term BBR-treatment of high-fat diet (HFD)-fed rats and mice (Xie et al., 2011; Zhang et al., 2012; Zhang et al., 2015b). No significant changes were observed in the major phyla of mice on a normal chow diet after short term BBR-treatment (Supplementary Fig. S2). However, significant shifts in the *Firmicutes* to *Bacteroidetes* ratio were observed after 5 days BBR treatment (Fig. 5A). Moreover, BBR treatment decreased levels of the genus *Clostridium* cluster XIVa and *Clostridium* cluster IV (Fig. 5A), which is consistent with a significantly lower fecal BSH activity (Fig. 5B). In addition, 3D PCA scores plot from urine global analysis showed distinct, time-dependent clustering of metabolites after BBR treatment (Supplementary Fig. 3). Urine metabolomics analysis revealed

that BBR treatment was associated with decreased levels of common microbial metabolites including hippurate, indoxyl sulfate, phenylacetylglycine (PAG) (Fig. 5C-D). These data are consistent with the observation of decreased genus *Clostridium*, which is involved in the production of microbial metabolites often found in urine (Lord and Bralley, 2008; Lees et al., 2013). However, fecal changes were not as significant as that found in urine, although a decreasing trend of butyrate and propionate and significant increase of glucose after 5 days BBR treatment was observed (Supplementary Fig. 4).

The antibiotic effect of BBR treatment on cecal bacteria in vitro

BBR is well-known as an effective antimicrobial compound used in the treatment of microbial infections (Yu et al., 2005; Bandyopadhyay et al., 2013). To investigate the direct effect of BBR on the gut microbiota, we used an in vitro model to assess the metabolic activity or membrane damage in bacteria using three doses of BBR. We determined the state of bacterial physiology using four different dyes: a dye that stains all cells (SybrGreen I); an impermeable dye that stains only dead or damaged cells (Pi); a cell permeable dye for cellular enzymatic activity (CFDA); and an oxonol dye for loss of membrane polarity ($DiBAC_4$) (Joux and Lebaron, 2000; Maurice et al., 2013; Maurice and Turnbaugh, 2013). BBR caused a significant dose-dependent increase in Pi positive bacteria from 17.4 ± 2.1% to 26.0 ± 1.3% and significantly decreased SybrGreen stained bacteria with high dose of BBR treatment (Fig. 6A-B). Furthermore, the significant dose-dependent increase in bacteria with LNA content and decreased HNA content were observed with BBR treatment (Fig. 6A). Three doses of BBR treatment all resulted in significant decreases in CFDA stained bacteria (Fig. 6B), which indicated decreased metabolic activity of bacterial cells with BBR treatment. Moreover, a significant increase in $DiBAC_4$ stained bacteria was observed with high dose of BBR treatment (Fig. 6B).

To investigate the changes in the composition of bacteria by BBR directly, qPCR bacterial quantification was performed on isolated bacterial DNA. BBR treatment resulted in dose-dependent decrease in numbers of bacteria from *Firmicutes* and *Clostridium* XIVa and increase in ratio of *Firmicutes*/*Bacteriodetes* (Fig. 7A and Supplementary Fig. S5). No significant changes in other phyla levels including *Bacteroidetes* or *Actinobacteria* were observed after BBR treatment (Supplementary Fig. S5).

^{1}H NMR-based metabolomics was employed to evaluate the direct metabolic impact of BBR on the intestinal microbiota. 3D PCA scores plot showed distinct clustering of bacteria with three doses of BBR treatment (Supplementary Fig. S6). Acetate, propionate and butyrate are the end metabolites of fermentation of dietary fiber by the gut microbiota (Den Besten et al., 2013). BBR treatment resulted in significantly lower butyrate and propionate levels but higher acetate and glucose levels in bacteria (Fig. 7C). Moreover, the levels of bacterial gene butyryl-CoA:acetate CoA-transferase (*but*) associated with butyrate production were significantly lower with middle and high doses of BBR treatment (Fig. 7B). Taken together, these observations indicate that BBR affects bacteria directly.

Discussion

This study demonstrated that remodeling of the intestinal microbiota by BBR leads to alteration of bile acid levels and activation of FXR signaling (Fig. 8). The effect of BBR on the gut microbiota of HFD-fed rats identified a marked decrease in the gut microbiota diversity and a phylum-shift of the gut bacteria in rats (Zhang et al., 2012; Zhang et al., 2015b). In this study, 5 days of oral BBR treatment of normal weight mice led to a significant change in the *Firmicutes* to *Bacteroidetes* ratio and reduced the genus *Clostridium*. These data indicated that the effects of BBR on the gut microbiota are dependent on diet and length of dosing. Furthermore, BBR treatment decreased levels of mouse urine microbial metabolites including hippurate, PAG, and indoxyl sulfate, which are in agreement with the observation of reduced *Clostridium* spp (Lord and Bralley, 2008; Tian et al., 2018).

The direct activity of BBR on the intestinal bacteria was observed in vitro using NMR-based metabolomics combined with flow cytometry. In vitro, BBR treatment lead to a dose-dependent increase in cell damage and decreased metabolic activity in bacteria, which is consistent with previous studies that have shown the effective antibacterial activity of BBR in vitro and in vivo (Yu et al., 2005; Bandyopadhyay et al., 2013). Furthermore, BBR treatment led to decreased HNA cells with higher metabolic activity and growth rates (Wang et al., 2009). Moreover, BBR treatment resulted in dose-dependent decrease in *Firmicutes* and *Clostridium* XIVa but no significant change in *Bacteroidetes* or *Actinobacteria* was observed, which supports our observation of reduced *Clostridium* by BBR treatment in vivo. This is consistent with reports that found active and damaged subsets in bacteria belong to *Firmicutes* and 90% of the affected OTUs were *Firmicutes* after antibiotics exposure (Maurice et al., 2013). Moreover, BBR treatment decreased the levels of bacterial butyrate-producing gene *but* and altered bacterial metabolite

levels including reduced levels of butyrate and propionate and increased acetate and glucose levels in vitro. These results indicated inhibition of bacterial fermentation by BBR treatment (Morrison et al., 2006; Vital et al., 2014). Collectively, the data suggest that BBR influences microbial metabolism.

The increased levels of taurine-conjugated bile acids with BBR treatment likely is a combination of both host and bacteria changes. The significantly higher levels of taurine-conjugated bile acids were observed in the liver, ileum, and feces after BBR treatment. Consistently, previous studies also indicated increased levels of taurine–conjugated bile acids in colon, ileum, and serum by intestine-restricted FXR agonist fexaramine (Pathak et al., 2018). An increase in gene expression involved in conjugation enzymes was observed in the host after BBR treatment, which indicated that BBR increased host bile acid conjugation pathways (Guo et al., 2016). Additionally, the increased levels of taurine-conjugated bile acids with BBR treatment is also associated with reducing *Clostridium* and its BSH activity. BSH is a bacterial enzyme that catalyzes the deconjugation of conjugated bile acids (Kumar et al., 2006). Among the *Firmicutes*, BSH activity has been detected in the genus *Lactobacillus* and *Clostridium* (Begley et al., 2006). A recent study indicated that tempol reduced the genus *Lactobacillus* and its BSH activity resulting in increased levels of taurine conjugated bile acids (Li et al., 2013). On the basis of these findings, the decreased BSH activity may result from the reduction or direct killing of *Clostridium* by BBR treatment. Moreover, the lower BSH activity contributed to the accumulation of taurine-conjugated bile acids in the BBR treatment group.

Activation of intestinal FXR by BBR exposure was associated with the accumulation of TCA. Previous studies showed that bile acid can activate ileal FXR, which simulated FGF15 in liver and elevated serum FGF15 (Li et al., 2018). One possible explanation for our results is that

activation of intestinal FXR by BBR treatment was associated with a marked accumulation of TCA. This is consistent with studies that found both BBR and TCA treatment activated FXR signaling in the intestine and exerted its lipid-lowering effect (Sun et al., 2017). FXR is a bile acid receptor and plays an key role in the regulation of bile acid metabolism (Forman et al., 1995) and tissue-restricted FXR activation was reported as a new therapeutic angle for obesity and related metabolic diseases (Fang et al., 2015; Pathak et al., 2018). Future work is still needed to investigate whether the same effect of BBR on microbiota occurs in obese or diabetic mice.

In summary, the effect of BBR on gut bacteria was studied using both in vitro and in vivo models. BBR reduced *Clostridium* and its BSH activity leading to the accumulation of TCA. The accumulation of TCA was associated with the activation of intestinal FXR. Our data provide new insights for studying the link between the microbiota, nuclear receptor signaling, and xenobiotics.

ACKNOWLEDGMENTS

We would like to thank Mr. Nelson Thomas Peterson for technical help and Dr. Frank J. Gonzalez for critical discussion of the data.

AUTHORSHIP CONTRIBUTIONS

Participated in research design: Tian, Patterson.

Conducted experiments: Tian, Cai, Gui, Nichols, Zhang, Mallappa.

Performed data analysis: Tian, Koo, Patterson.

Wrote or contributed to the writing of the manuscript: Tian, Patterson.

REFERENCES

Ali AH, Carey EJ, and Lindor KD (2015) Recent advances in the development of farnesoid X receptor agonists. *Ann Transl Med* **3:**5.

Arab JP, Karpen SJ, Dawson PA, Arrese M, and Trauner M (2017) Bile acids and nonalcoholic fatty liver disease: molecular insights and therapeutic perspectives. *Hepatology* **65:**350-362.

Bandyopadhyay S, Patra PH, Mahanti A, Mondal DK, Dandapat P, Bandyopadhyay S, Samanta I, Lodh C, Bera AK, Bhattacharyya D, Sarkar M, and Baruah KK (2013) Potential antibacterial activity of berberine against multi drug resistant enterovirulent *Escherichia coli* isolated from yaks (*Poephagus grunniens*) with haemorrhagic diarrhoea. *Asian Pac J Trop Med* **6:**315-319.

Begley M, Hill C, and Gahan CGM (2006) Bile salt hydrolase activity in probiotics. *Appl Environ Microb* **72:**1729-1738.

Chen CQ, Tao CH, Liu ZC, Lu ML, Pan QH, Zheng LJ, Li Q, Song ZS, and Fichna J (2015) A randomized clinical trial of berberine hydrochloride in patients with diarrhea-predominant irritable bowel syndrome. *Phytother Res* **29:**1822-1827.

Cyphert HA, Ge XM, Kohan AB, Salati LM, Zhang YQ, and Hillgartner FB (2012) Activation of the farnesoid X receptor induces hepatic expression and secretion of fibroblast growth factor 21. *J Biol Chem* **287:**25123-25138.

Dawson PA, Lan T, and Rao A (2009) Bile acid transporters. *J Lipid Res* **50:**2340-2357.

Den Besten G, Van Eunen K, Groen AK, Venema K, Reijngoud DJ, and Bakker BM (2013) The role of short-chain fatty acids in the interplay between diet, gut microbiota, and host energy metabolism. *J Lipid Res* **54:**2325-2340.

Duran-Sandoval D, Mautino G, Martin GV, Percevault F, Barbier O, Fruchart JC, Kuipers F, and Staels B (2004) Glucose regulates the expression of the farnesoid X receptor in liver. *Diabetes* **53:**890-898.

Fang S, Suh JM, Reilly SM, Yu E, Osborn O, Lackey D, Yoshihara E, Perino A, Jacinto S, Lukasheva Y, Atkins AR, Khvat A, Schnab B, Yu RT, Brenner DA, Coulter S, Liddle C, Schoonjans K, Olefsky JM, Saltiel AR, Downes M, and Evans RM (2015) Intestinal FXR agonism promotes adipose tissue browning and reduces obesity and insulin resistance. *Nat Med* **21:**71-77.

Forman BM, Goode E, Chen J, Oro AE, Bradley DJ, Perlmann T, Noonan DJ, Burka LT, McMorris T, Lamph WW, Evans RM, and Weinberger C (1995) Identification of a nuclear receptor that is activated by farnesol metabolites. *Cell* **81:**687-693.

Geier A, Wagner M, Dietrich CG, and Trauner M (2007) Principles of hepatic organic anion transporter regulation during cholestasis, inflammation and liver regeneration. *BBA Mol Cell Res* **1773:**283-308.

Guo Y, Zhang YC, Huang WH, Selwyn FP, and Klaassen CD (2016) Dose-response effect of berberine on bile acid profile and gut microbiota in mice. *Bmc Complement Altern Med* **16:**394.

Han JL, Lin HL, and Huang WP (2011) Modulating gut microbiota as an anti-diabetic mechanism of berberine. *Med Sci Monitor* **17:**RA164-RA167.

Inagaki T, Moschetta A, Lee YK, Peng L, Zhao GX, Downes M, Yu RT, Shelton JM, Richardson JA, Repa JJ, Mangelsdorf DJ, and Kliewer SA (2006) Regulation of antibacterial defense in the small intestine by the nuclear bile acid receptor. *P Natl Acad Sci USA* **103:**3920-3925.

Jiang CT, Xie C, Li F, Zhang LM, Nichols RG, Krausz KW, Cai JW, Qi YP, Fang ZZ, Takahashi S, Tanaka N, Desai D, Amin SG, Albert I, Patterson AD, and Gonzalez FJ (2015a) Intestinal farnesoid X receptor signaling promotes nonalcoholic fatty liver disease. *J Clin Invest* **125:**386-402.

Jiang CT, Xie C, Lv Y, Li J, Krausz KW, Shi JM, Brocker CN, Desai D, Amin SG, Bisson WH, Liu YL, Gavrilova O, Patterson AD, and Gonzalez FJ (2015b) Intestine-selective farnesoid X receptor inhibition improves obesity-related metabolic dysfunction. *Nat Commun* **6:**10166.

Jiang LM, Huang J, Wang YL, and Tang HR (2012) Eliminating the dication-induced intersample chemical-shift variations for NMR-based biofluid metabonomic analysis. *Analyst* **137:**4209-4219.

Joux F and Lebaron P (2000) Use of fluorescent probes to assess physiological functions of bacteria at single-cell level. *Microbes Infect* **2:**1523-1535.

Kawamata Y, Fujii R, Hosoya M, Harada M, Yoshida H, Miwa M, Fukusumi S, Habata Y, Itoh T, Shintani Y, Hinuma S, Fujisawa Y, and Fujino M (2003) A G protein-coupled receptor responsive to bile acids. *J Biol Chem* **278:**9435-9440.

Kong WJ, Wei J, Abidi P, Lin MH, Inaba S, Li C, Wang YL, Wang ZZ, Si SY, Pan HN, Wang SK, Wu JD, Wang Y, Li ZR, Liu JW, and Jiang JD (2004) Berberine is a novel cholesterol-lowering drug working through a unique mechanism distinct from statins. *Nat Med* **10:**1344-1351.

Kumar RS, Brannigan JA, Prabhune AA, Pundle AV, Dodson GG, Dodson EJ, and Suresh CG (2006) Structural and functional analysis of a conjugated bile salt hydrolase from Bifidobacterium longum reveals an evolutionary relationship with penicillin V acylase. *J Biol Chem* **281:**32516-32525.

Lambert G, Amar MJA, Guo G, Brewer HB, Gonzalez FJ, and Sinal CJ (2003) The farnesoid X-receptor is an essential regulator of cholesterol homeostasis. *J Biol Chem* **278:**2563-2570.

Lees HJ, Swann JR, Wilson ID, Nicholson JK, and Holmes E (2013) Hippurate: the natural history of a mammalian-microbial ometabolite. *J Proteome Res* **12:**1527-1546.

Lefebvre P, Cariou B, Lien F, Kuipers F, and Staels B (2009) Role of bile acids and bile acid receptors in metabolic regulation. *Physiol Rev* **89:**147-191.

Li F, Jiang CT, Krausz KW, Li YF, Albert I, Hao HP, Fabre KM, Mitchell JB, Patterson AD, and Gonzalez FJ (2013) Microbiome remodelling leads to inhibition of intestinal farnesoid X receptor signalling and decreased obesity. *Nat Commun* **4:**2384.

Li Q, Zhao Q, Zhang CZ, Zhang P, Hu AB, Zhang LJ, Schroder PM, Ma Y, Guo ZY, Zhu XF, and He XS (2018) The ileal FGF15/19 to hepatic FGFR4 axis regulates liver regeneration after partial hepatectomy in mice. *J Physiol Biochem* **74:**247-260.

Li TG and Chiang JYL (2013) Nuclear receptors in bile acid metabolism. *Drug Metab Rev* **45:**145-155.

Lord RS and Bralley JA (2008) Clinical applications of urinary organic acids. Part 2. dysbiosis markers. *Alternat Med Rev* **13:**292-306.

Maurice CF, Haiser HJ, and Turnbaugh PJ (2013) Xenobiotics shape the physiology and gene expression of the active human gut microbiome. *Cell* **152:**39-50.

Maurice CF and Turnbaugh PJ (2013) Quantifying and identifying the active and damaged subsets of indigenous microbial communities, in: *Microbial Metagenomics, Metatranscriptomics, and Metaproteomics* (DeLong EF ed), pp 91-107.

Morrison DJ, Mackay WG, Edwards CA, Preston T, Dodson B, and Weaver LT (2006) Butyrate production from oligofructose fermentation by the human faecal flora: what is the contribution of extracellular acetate and lactate? *Brit J Nutr* **96:**570-577.

Pathak P, Xie C, Nichols RG, Ferrell JM, Boehme S, Krausz KW, Patterson AD, Gonzalez FJ, and Chiang JYL (2018) Intestine farnesoid X receptor agonist and the gut microbiota activate G-protein bile acid receptor-1 signaling to improve metabolism. *Hepatology*.

Ridlon JM, Kang DJ, Hylemon PB, and Bajaj JS (2014) Bile acids and the gut microbiome. *Curr Opin Gastroe* **30:**332-338.

Sayin SI, Wahlstrom A, Felin J, Jantti S, Marschall HU, Bamberg K, Angelin B, Hyotylainen T, Oresic M, and Backhed F (2013) Gut microbiota regulates bile acid metabolism by reducing the levels of tauro-beta-muricholic Acid, a naturally occurring FXR antagonist. *Cell Metab* **17:**225-235.

Sun RB, Yang N, Kong B, Cao B, Feng D, Yu XY, Ge C, Huang JQ, Shen JL, Wang P, Feng SQ, Fei F, Guo JH, He J, Aa N, Chen Q, Pan Y, Schumacher JD, Yang CS, Guo GL, Aa JY, and Wang GJ (2017) Orally

administered berberine modulates hepatic lipid metabolism by altering microbial bile acid metabolism and the intestinal FXR signaling pathway. *Mol Pharmacol* **91:**110-122.

Tang J, Feng YB, Tsao S, Wang N, Curtain R, and Wang YW (2009) Berberine and Coptidis Rhizoma as novel antineoplastic agents: a review of traditional use and biomedical investigations. *J Ethnopharmacol* **126:**5-17.

Tian Y, Nichols RG, Cai JW, Patterson AD, and Cantorna MT (2018) Vitamin A deficiency in mice alters host and gut microbial metabolism leading to altered energy homeostasis. *J Nutr Biochem* **54:**28-34.

Vital M, Howe AC, and Tiedje JM (2014) Revealing the bacterial butyrate synthesis pathways by analyzing (Meta) genomic data. *mBio* **5:**e00889-00814.

Wang YY, Hammes F, Boon N, Chami M, and Egli T (2009) Isolation and characterization of low nucleic acid (LNA)-content bacteria. *ISME J* **3:**889-902.

Xie WD, Gu DY, Li JN, Cui K, and Zhang YO (2011) Effects and action mechanisms of berberine and rhizoma coptidis on gut microbes and obesity in high-fat diet-fed C57BL/6J Mice. *Plos One* **6:**e24520.

Xu JH, Liu XZ, Pan W, and Zou DJ (2017) Berberine protects against diet-induced obesity through regulating metabolic endotoxemia and gut hormone levels. *Mol Med Rep* **15:**2765-2787.

Yu HH, Kim KJ, Cha JD, Kim HK, Lee YE, Choi NY, and You YO (2005) Antimicrobial activity of berberine alone and in combination with ampicillin or oxacillin against methicillin-resistant Staphylococcus aureus. *J Med Food* **8:**454-461.

Zhang LM, Nichols RG, Correll J, Murray IA, Tanaka N, Smith PB, Hubbard TD, Sebastian A, Albert I, Hatzakis E, Gonzalez FJ, Perdew GH, and Patterson AD (2015a) Persistent organic pollutants modify gut microbiota-host metabolic homeostasis in mice through aryl hydrocarbon receptor activation. *Environ Health Perspect* **123:**679-688.

Zhang LM, Xie C, Nichols RG, Chan SHJ, Jiang CT, Hao RX, Smith PB, Cai JW, Simons MN, Hatzakis E, Maranas CD, Gonzalez FJ, and Patterson AD (2016) Farnesoid X receptor signaling shapes the gut microbiota and controls hepatic lipid metabolism. *Msystems* **1:**e00070-00016.

Zhang X, Zhao YF, Xu J, Xue ZS, Zhang MH, Pang XY, Zhang XJ, and Zhao LP (2015b) Modulation of gut microbiota by berberine and metformin during the treatment of high-fat diet-induced obesity in rats. *Sci Rep* **5:**14405.

Zhang X, Zhao YF, Zhang MH, Pang XY, Xu J, Kang CY, Li M, Zhang CH, Zhang ZG, Zhang YF, Li XY, Ning G, and Zhao LP (2012) Structural Changes of Gut Microbiota during Berberine-Mediated Prevention of Obesity and Insulin Resistance in High-Fat Diet-Fed Rats. *Plos One* **7:**e42529.

Zhang YQ, Lee FY, Barrera G, Lee H, Vales C, Gonzalez FJ, Willson TM, and Edwards PA (2006) Activation of the nuclear receptor FXR improves hyperglycemia and hyperlipidemia in diabetic mice. *P Natl Acad Sci USA* **103:**1006-1011.

Zhang ZG, Zhang HZ, Li B, Meng XJ, Wang JQ, Zhang YF, Yao SS, Ma QY, Jin LN, Yang J, Wang WQ, and Ning G (2014) Berberine activates thermogenesis in white and brown adipose tissue. *Nat Commun* **5:**5493.

FOOTNOTES

This work was supported in part by the Pennsylvania Department of Health using Tobacco CURE Funds; the National Institutes of Health T32 LM 12415-1; the National Institute of Food and Agriculture, U.S. Department of Agriculture, under award number 2914-38420-21822.

FIGURE LEGENDS

Fig. 1 Scheme for determining the effects of BBR in vivo (A) and vitro (B).

Fig. 2 (A-D) Quantification of bile acids in feces (A), liver (B), ileum (C), and total (D) from mice after 5 days vehicle or BBR treatment. (E) qPCR analysis of mRNA encoding bile acid synthesis in the liver from mice after 5 days vehicle or BBR treatment. Values are the median and interquartile ranges of n = 6 per group. *$p < 0.05$, **$p < 0.01$. Abbreviations: CA, cholic acid; DCA, deoxycholic acid; LCA, lithocholic acid; UDCA, ursodeoxycholic acid; CDCA, chenodeoxycholic acid; MCA, muricholic acid; T, taurine-conjugated species. Hyocholic acid (HCA), ursocholanic acid, lithocholenic acid, isolithocholenic acid, allolithocholenic acid, hyodexycholic acid, isodexycholic acid, tauro-ursocholanic acid, 3,7,12 tauro-dehydrocholic acid, TαMCA, TLCA, THCA were measured that under detection limit in this study.

Fig. 3 (A) qPCR analysis of *Fgf15*, *Fxr,* and *Shp* mRNAs in the ileum and *Fxr* and *Shp* mRNA expression in the liver from mice after 5 days vehicle or BBR treatment. (B) qPCR analysis of mRNA encoding bile acid conjugation and transporters in the liver and ileum from mice after 5 days vehicle or BBR treatment. Values are the median and interquartile ranges of n = 6 per group. *$p < 0.05$

Fig. 4 Luciferase assays of the activation of FXR by 100 μM TCA, TCDCA, TUDCA, TβMCA, and BBR. Values are the mean ± SD of n = 3 per group. ****$p < 0.0001$

Fig. 5 (A) qPCR analysis of *Firmicutes*/*Bacteroidetes*, *Clostridium* XIVa, and *Clostridium* IV in the cecal contents from mice after 5 days vehicle or BBR treatment. (B) Fecal BSH enzyme activity after BBR 5 days vehicle or BBR treatment. (C) OPLS-DA scores plot (left) and coefficient plot (right) derived from ^{1}H NMR spectra of urine samples from mice after 5 days vehicle (■) or BBR (●) treatment. The model was evaluated with CV-ANOVA with $p = 0.021$. (D) Relative abundance of urine bacterial metabolites measured by ^{1}H NMR data from mice after 0, 1, 3, and 5 days BBR treatment. Values are the median and interquartile ranges of n = 6 per group. *$p < 0.05$. Abbreviations: DMA, dimethylamine; TMA, trimethylamine; PAG, phenylacetylglycine.

Fig. 6 Flow cytometric analyses of proportions of SybrGreen I, LNA, and HNA (A), Pi, $DiBAC_4$, and CFDA (B) cells from cecal bacteria with vehicle or three doses BBR treatment. Values are the mean ± SD of n = 5 per group. * $p < 0.05$, ** $p < 0.01$, *** $p < 0.001$, **** $p < 0.0001$

Fig. 7 (A) qPCR analysis of *Firmicutes*/*Bacteroidetes*, *Clostridium* XIVa, *Clostridium* IV, and (B) bacterially produced butyryl-CoA:acetate CoA-transferase (*but*) from cecal bacteria with vehicle or three doses BBR treatment. (C) Acetate, propionate, butyrate, and glucose levels in the cecal bacteria with vehicle or three doses BBR treatment by ^{1}H NMR analysis. Values are the mean ± SD of n = 5 (flow cytometry) or 6 (qPCR and NMR) per group. * $p < 0.05$, ** $p < 0.01$, *** $p < 0.001$, **** $p < 0.0001$

Fig. 8 Remodeling of the gut microbiota by BBR leads to a change in the composition of bile acids and associated activation of FXR signaling. The metabolite, bacteria, enzyme, or mRNA in red or

blue represent a higher or lower level in the intestines obtained from BBR-treated mice compared to vehicle.

DMD Fast Forward. Published on November 8, 2018 as DOI: 10.1124/dmd.118.083691
This article has not been copyedited and formatted. The final version may differ from this version.

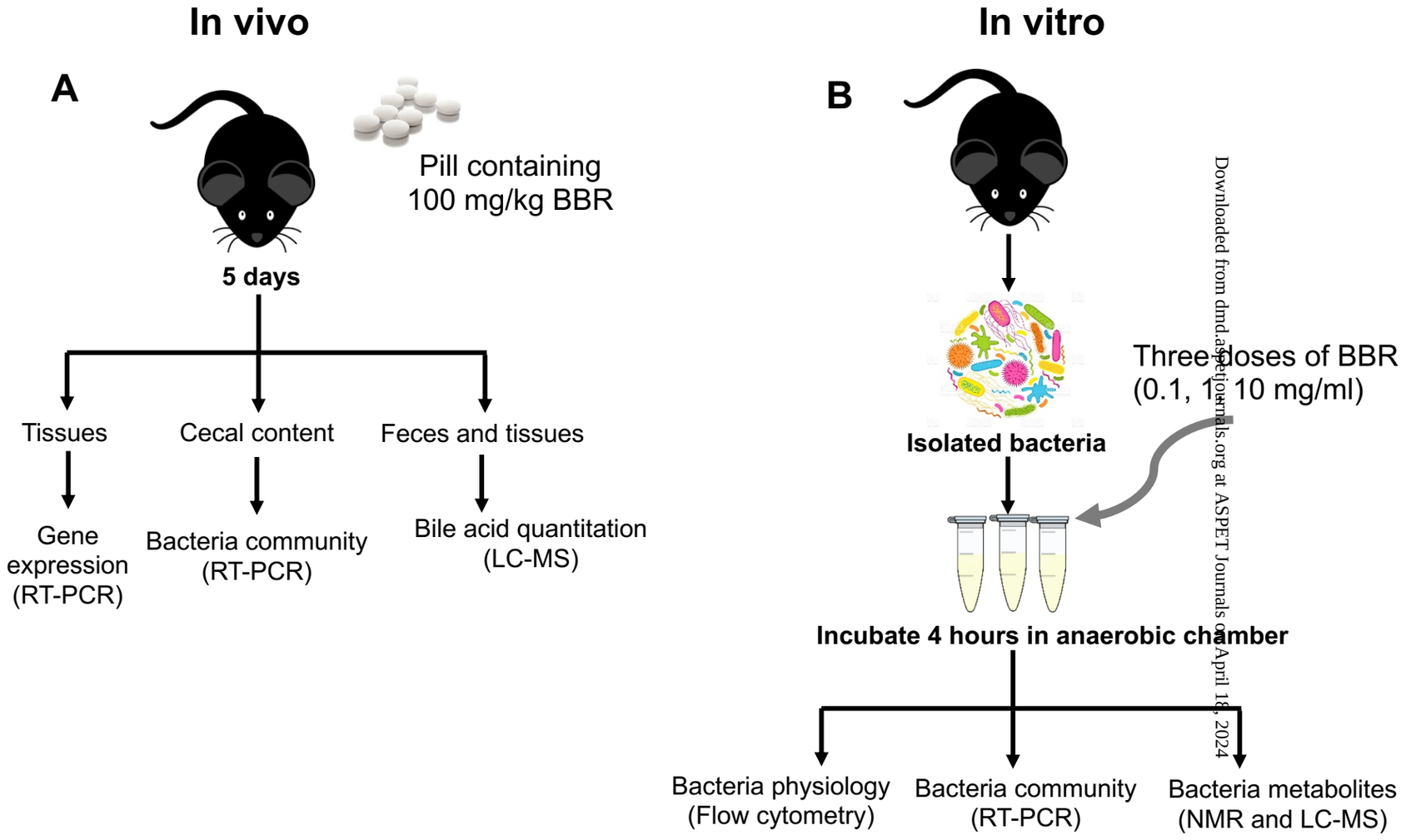

Fig. 1

DMD Fast Forward. Published on November 8, 2018 as DOI: 10.1124/dmd.118.083691
This article has not been copyedited and formatted. The final version may differ from this version.

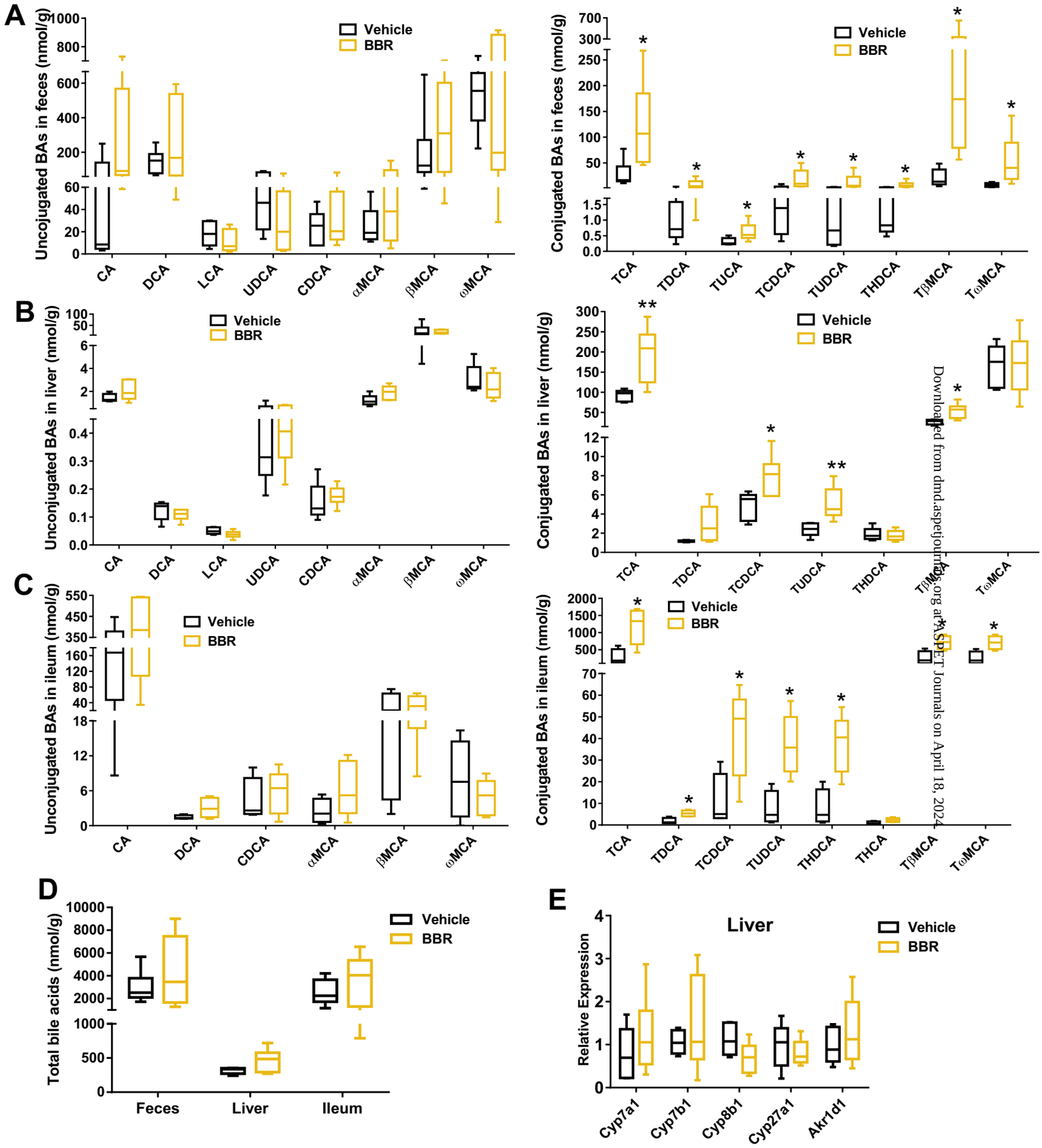

Fig. 2

DMD Fast Forward. Published on November 8, 2018 as DOI: 10.1124/dmd.118.083691
This article has not been copyedited and formatted. The final version may differ from this version.

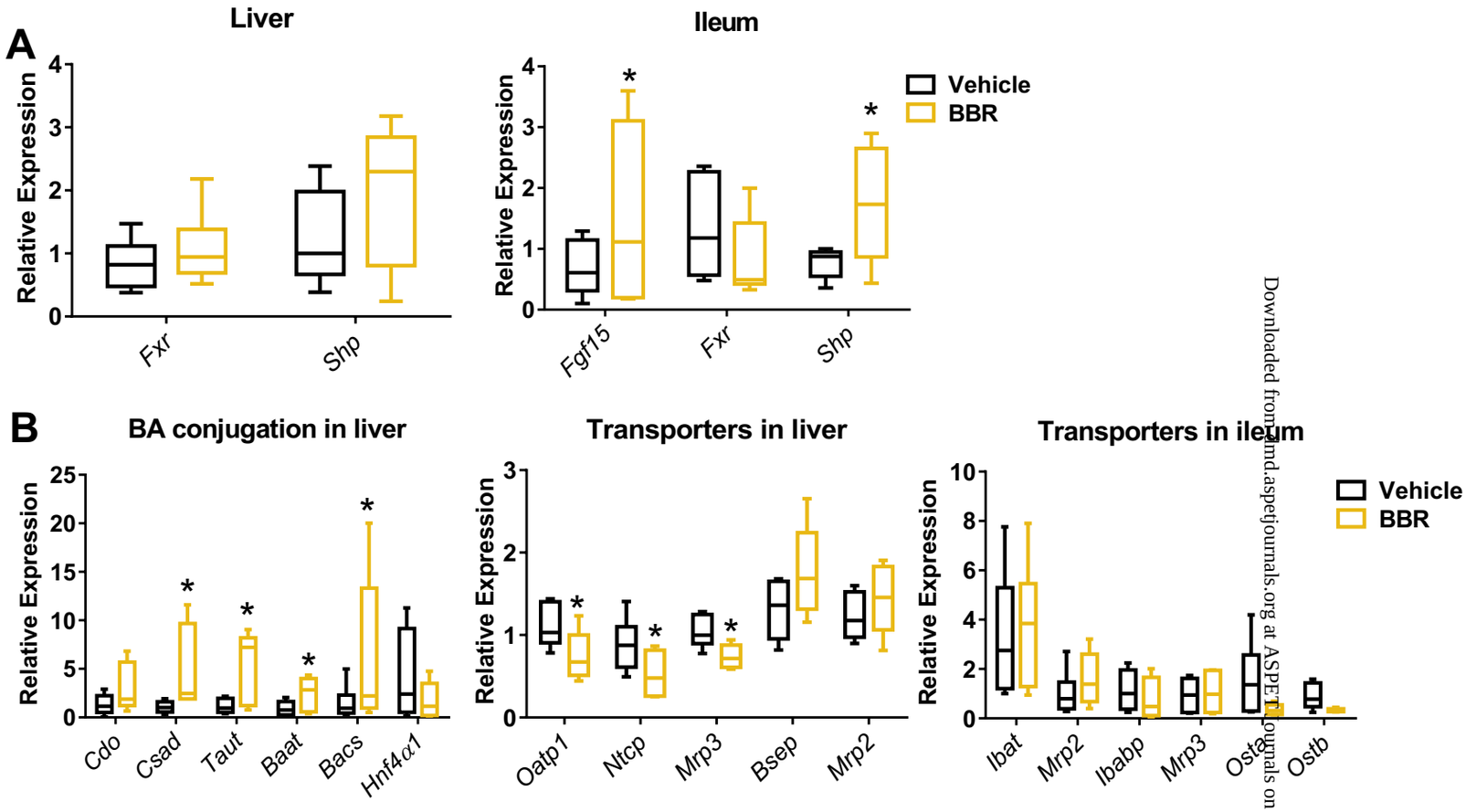

Fig. 3

DMD Fast Forward. Published on November 8, 2018 as DOI: 10.1124/dmd.118.083691
This article has not been copyedited and formatted. The final version may differ from this version.

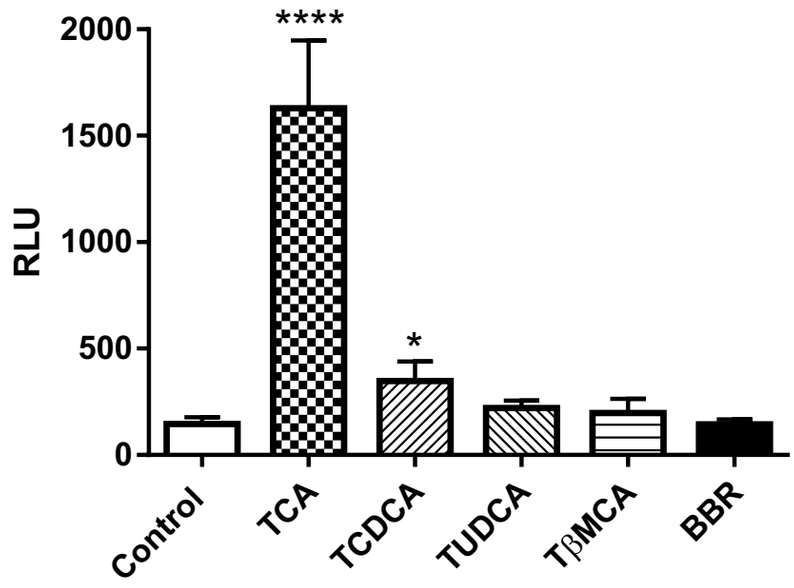

Fig. 4

DMD Fast Forward. Published on November 8, 2018 as DOI: 10.1124/dmd.118.083691
This article has not been copyedited and formatted. The final version may differ from this version.

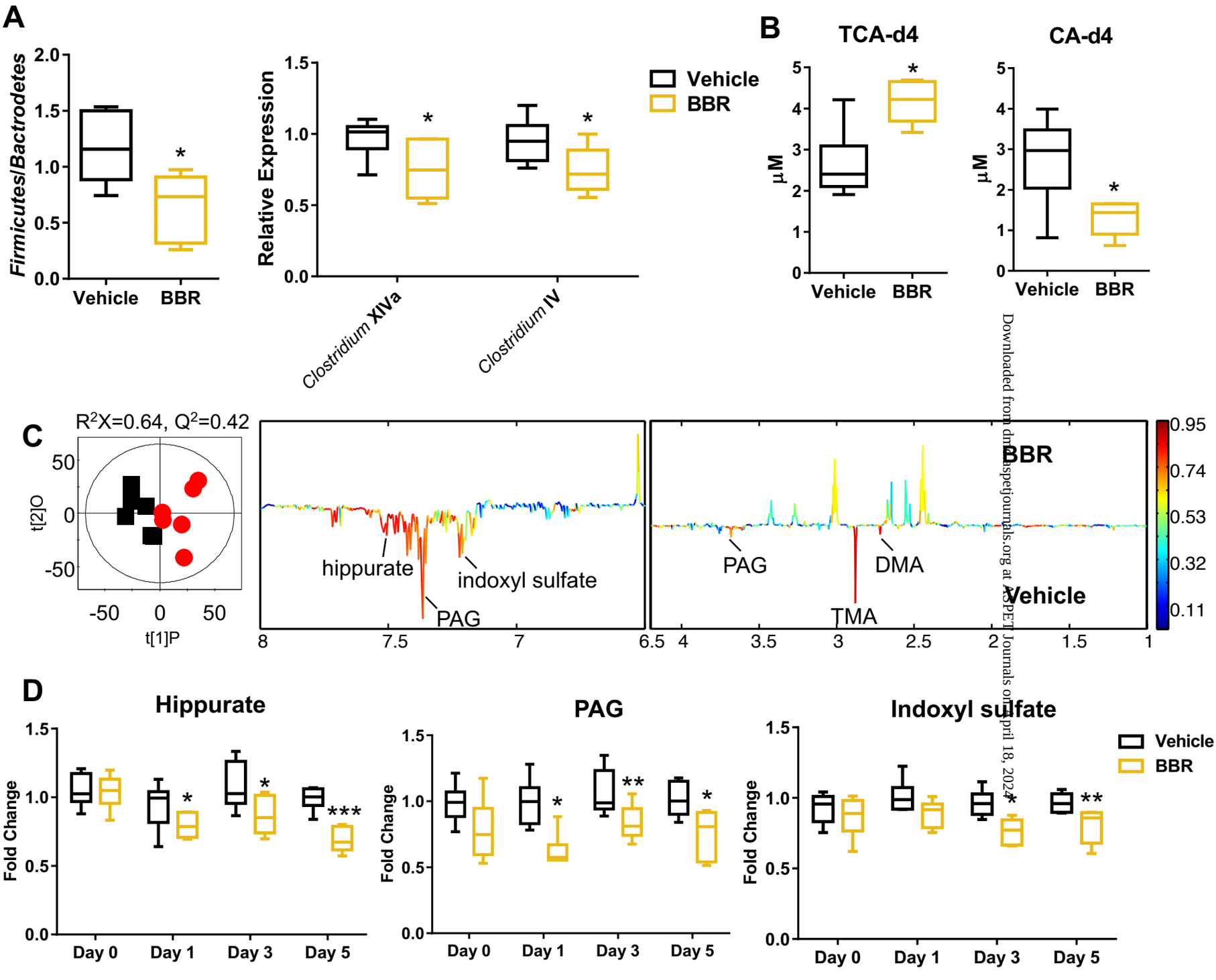

Fig. 5

DMD Fast Forward. Published on November 8, 2018 as DOI: 10.1124/dmd.118.083691
This article has not been copyedited and formatted. The final version may differ from this version.

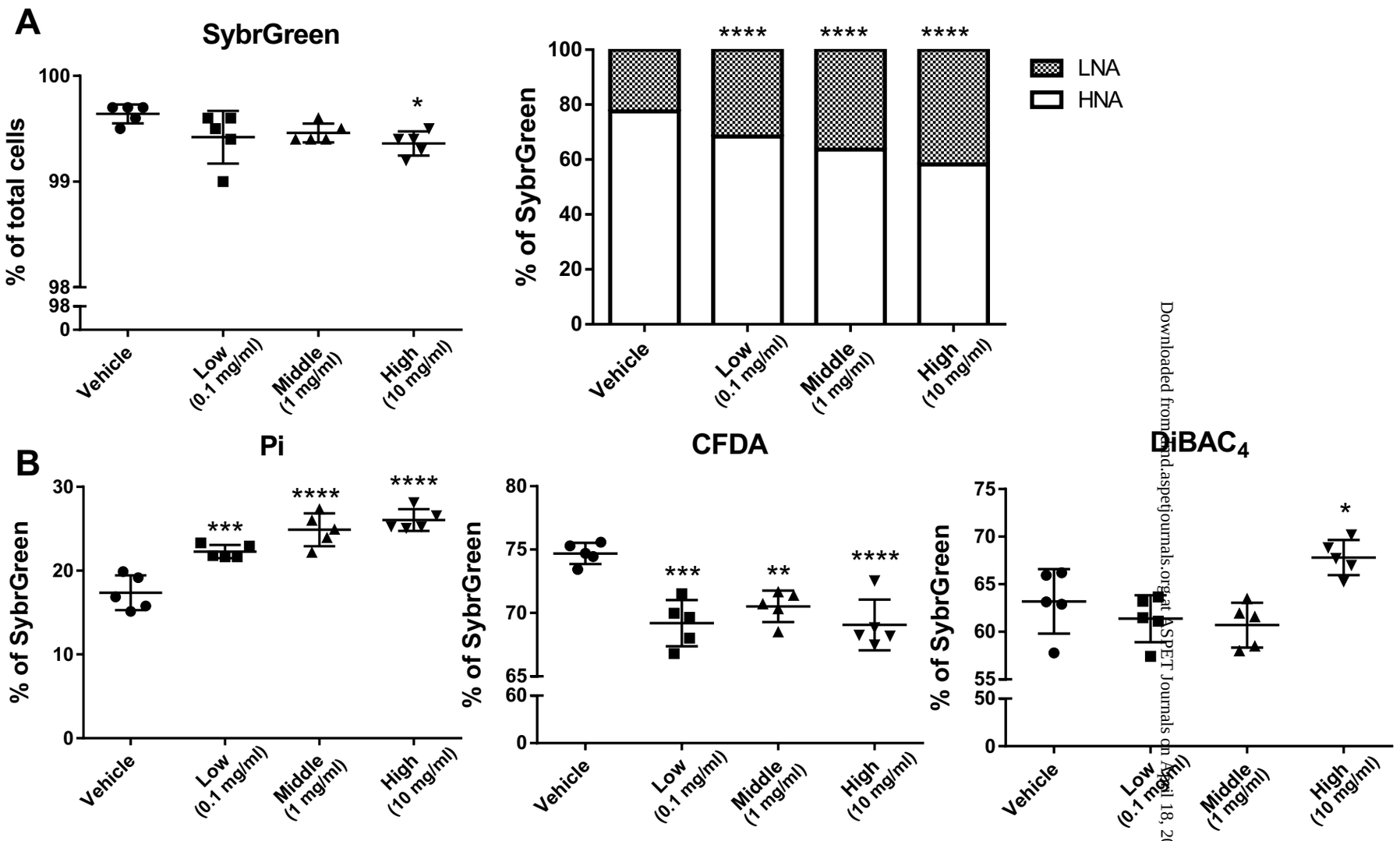

Fig. 6

DMD Fast Forward. Published on November 8, 2018 as DOI: 10.1124/dmd.118.083691
This article has not been copyedited and formatted. The final version may differ from this version.

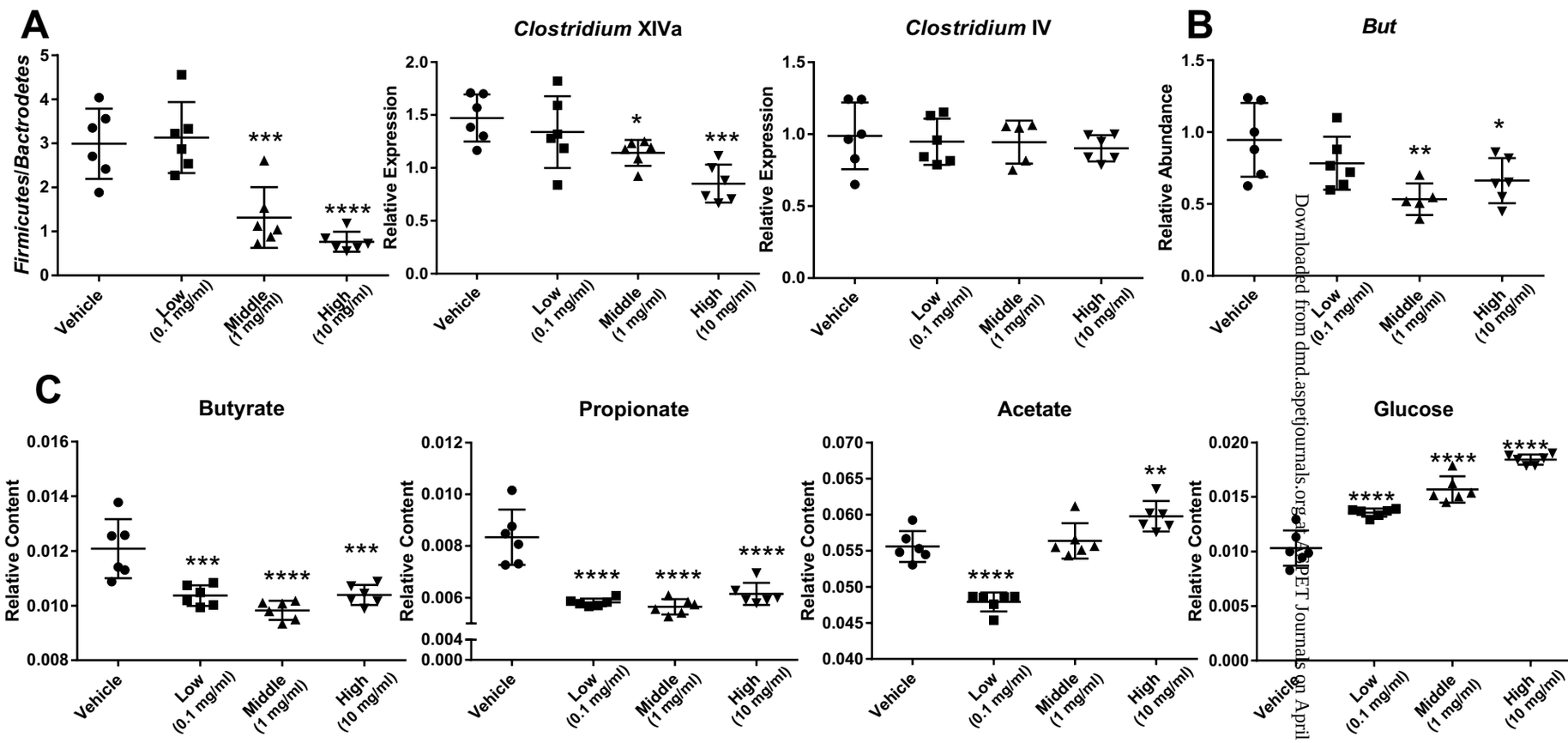

Fig. 7

DMD Fast Forward. Published on November 8, 2018 as DOI: 10.1124/dmd.118.083691
This article has not been copyedited and formatted. The final version may differ from this version.

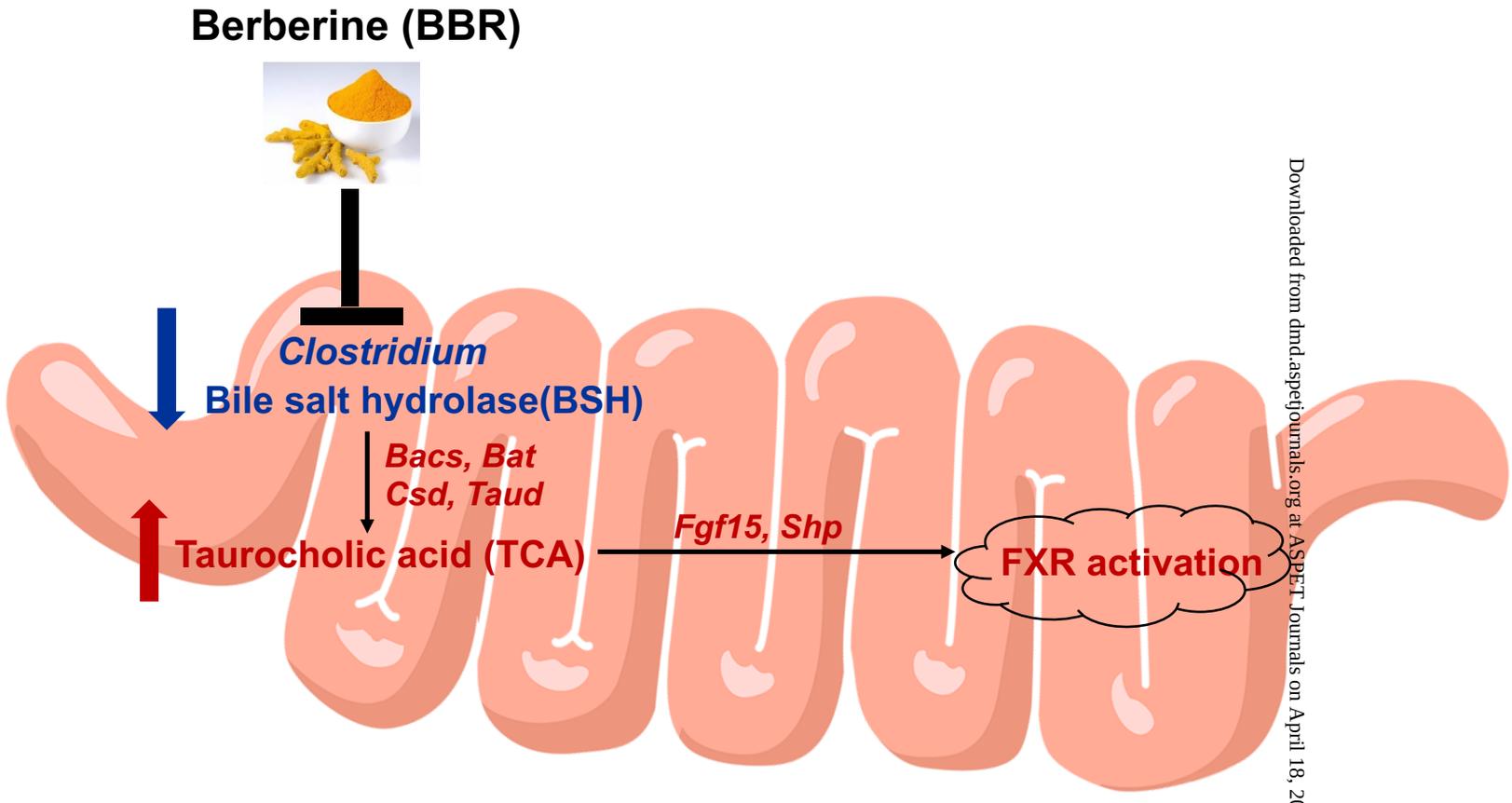

Fig. 8

Berberine Directly Impacts the Gut Microbiota to Promote Intestinal Farnesoid X Receptor Activation

Yuan Tian, Jingwei Cai, Wei Gui, Robert G. Nichols, Imhoi Koo, Jingtao Zhang, Mallappa Anitha, Andrew D. Patterson

Supplemental Table 1. mRNA gene-targeted primers used in this study

Gene	Abbreviation	Sequence (5'-3')
Farnesoid X receptor	*Fxr*	TCCAGGGTTTCAGACACTGG GCCGAACGAAGAAACATGG
Short heterodimer partner	*Shp*	CGATCCTCTTCAACCCAGATG AGGGCTCCAAGACTTCACACA
Fibroblast growth factor 15	*Fgf15*	ACGTCCTTGATGGCAATCG GAGGACCAAAACGAACGAAA
Cytochrome P450, family 7, subfamily A, polypeptide 1 (Cholesterol 7α-hydroxylase)	*Cyp7a1*	AGCAACTAAACAACCTGCCAGT ACTAGTCCGGATATTCAAGGATGCA
Cytochrome P450, family 7, subfamily B, polypeptide 1 (Oxysterol 7α-hydroxylase)	*Cyp7b1*	TAGCCCTCTTTCCTCCACTCATA GAACCGATCGAACCTAAATTCCT
Cytochrome P450, family 8, subfamily B, polypeptide 1 (Sterol 12α-hydroxylase)	*Cyp8b1*	GGCTGGCTTCCTGAGCTTATT ACTTCCTGAACAGCTCATCGG
Cytochrome P450, family 27, subfamily A, polypeptide 1 (Sterol 27-hydroxylase)	*Cyp27a1*	GCCTCACCTATGGGATCTTCA TCAAAGCCTGACGCAGATG
Aldo-keto reductase family 1 member D1	*Akr1d1*	TGCACACCACCAAATATCCCT CTTCACTGCCACATAGGTCTTC
Organic anion transporting protein 1	*Oatp1*	CAGTCTTACGAGTGTGCTCCAGAT ATGAGGAATACTGCCTCTGAAGTG
Na+/taurocholate cotransporter	*Ntcp*	ATGACCACCTGCTCCAGCTT GCCTTTGTAGGGCACCTTGT
Multidrug resistance-associated protein (Abcc3)	*Mrp3*	TCCCACTTTTCGGAGACAGTAAC ACTGAGGACCTTGAAGTCTTGGA
Multidrug resistance-associated protein (Abcc2)	*Mrp2*	GGATGGTGACTGTGGGCTGAT GGCTGTTCTCCCTTCTCATGG
Bile salt export pump (Abcb11)	*Bsep*	CTGCCAAGGATGCTAATGCA CGATGGCTACCCTTTGCTTCT
Cysteine dioxygenase	*Cdo*	GGGGACGAAGTCAACGTGG ACCCCAGCACAGAATCATCAG
Cysteine sulfinic acid decarboxylase	*Csad*	CCAGGACGTGTTTGGGATTGT ACCAGTCTTGACACTGTAGTGA
Taurine transporter	*Taut*	GCACACGGCCTGAAGATGA ATTTTTGTAGCAGAGGTACGGG
Bile acid-CoA: amino acid *N*-acyltransferase	*Baat*	GGAAACCTGTTAGTTCTCAGGC GTGGACCCCCATATAGTCTCC
Bile acid-CoA synthetase	*Bacs*	ACCCTGGATCAGCTCCTGGAT GTTCTCAGCTAGCAGCTTGG
Hepatic nuclear factor 4α1	*Hnf4α1*	AAATGTGCAGGTGTTGACCA CACGCTCCTCCTGAAGAATC
Ileal bile acid transporter	*Ibat*	ACCACTTGCTCCACACTGCTT CGTTCCTGAGTCAACCCACAT

Ileal bile acid-binding protein	*Ibabp*	CAGGAGACGTGATTGAAAGGG GCCCCCAGAGTAAGACTGGG
Organic solute transporter α	*Osta*	TGTTCCAGGTGCTTGTCATCC CCACTGTTAGCCAAGATGGAGAA
Organic solute transporter β	*Ostb*	GATGCGGCTCCTTGGAATTA GGAGGAACATGCTTGTCATGAC
Beta actin	*Actb*	AGAGGGAAATCGTGCGTGAC CAATAGTGATGACCTGGCCGT

Supplemental Table 2. 16S rRNA gene-targeted group-specific primers used in this study

Target bacterial group	Primer	Sequence (5'-3')
Universal	Eub338	ACT CCT ACG GGA GGC AGC AG
	Eub518	ATT ACC GCG GCT GCT GG
Firmicutes	Lgc353	GCA GTA GGG AAT CTT CCG
	Eub518	ATT ACC GCG GCT GCT GG
Bacteroidetes	Cfb319	GTA CTG AGA CAC GGA CCA
	Eub518	ATT ACC GCG GCT GCT GG
Actinobacteria	Actino235	CGC GGC CTA TCA GCT TGT TG
	Eub518	ATT ACC GCG GCT GCT GG
αProteobacteria	Eub338	ACT CCT ACG GGA GGC AGC AG
	Alf685	TCT ACG RAT TTC ACC YCT AC
βProteobacteria	Eub338	ACT CCT ACG GGA GGC AGC AG
	Bet680	TCA CTG CTA CAC GYG
Clostridium XIVa	G-Ccoc-F	AAA TGA CGG TAC CTG ACT AA
	G-Ccoc-R	CTT TGA GTT TCA TTC TTG CGA A
Clostridium IV	sg-Clept-F	GCA CAA GCA GTG GAG T
	sg-Clept-R3	CTT CCT CCG TTT TGT CAA

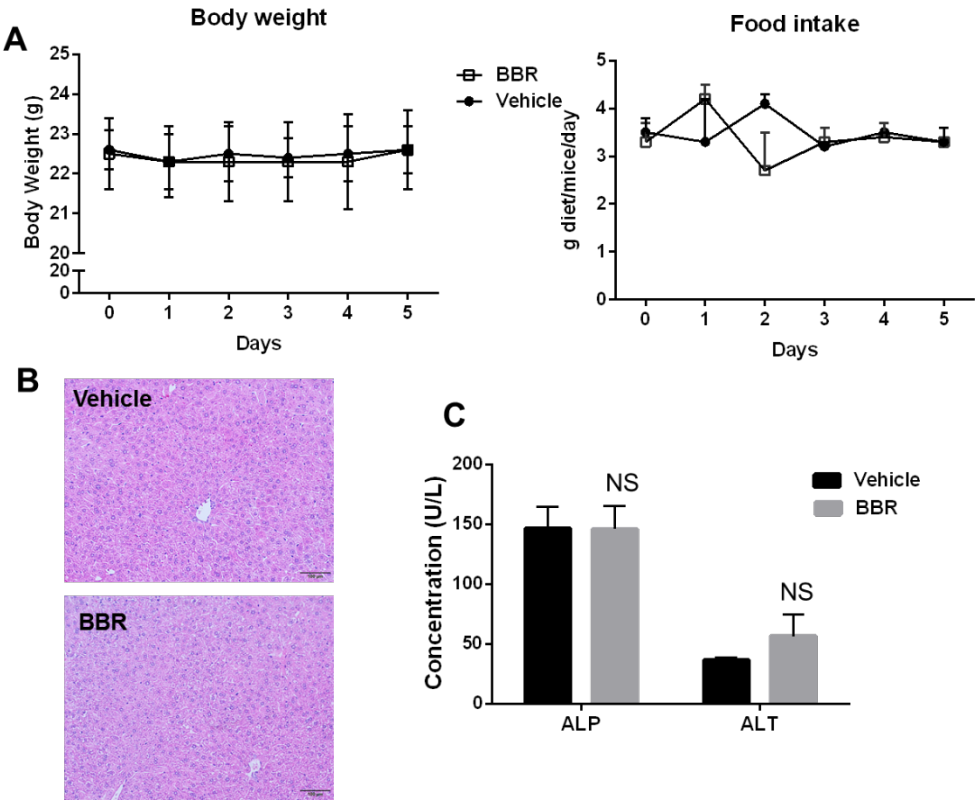

Supplemental Fig. 1 (A) The body weight and food intake of mice recorded every day during 5 days vehicle or BBR treatment. (B) Light microscopic examination of H&E-stained liver sections from mice after 5 days vehicle or BBR treatment. (C) serum concentrations of alanine transaminase (ALT) and alkaline phosphatase (ALP) from mice after 5 days vehicle or BBR treatment. Values are the mean ± SD of n = 6 per group.

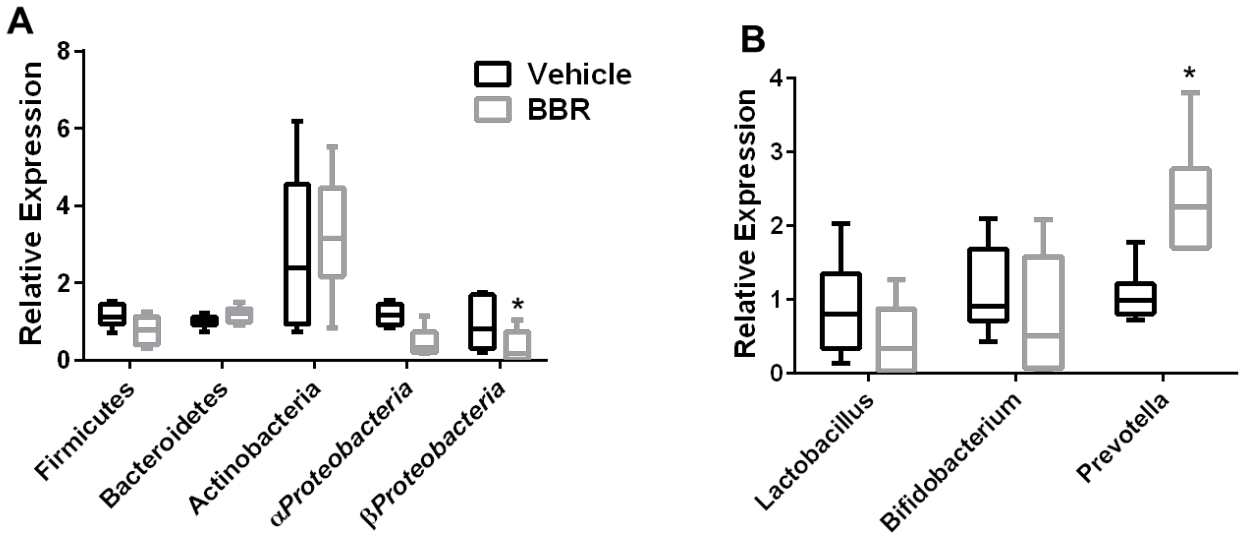

Supplemental Fig. 2 qPCR analysis of major phylum level bacteria including *Firmicutes, Bacteroidetes, Actinobacteria*, *Proteobacteria,* and *Proteobacteria* (A) and special species including *Lactobacillus*, *Bifidobacterium*, and *Prevotella* (B) in the cecal contents from mice after 5 days vehicle or BBR treatment. Values are the median and interquartile ranges of n = 6 per group. * $p < 0.05$

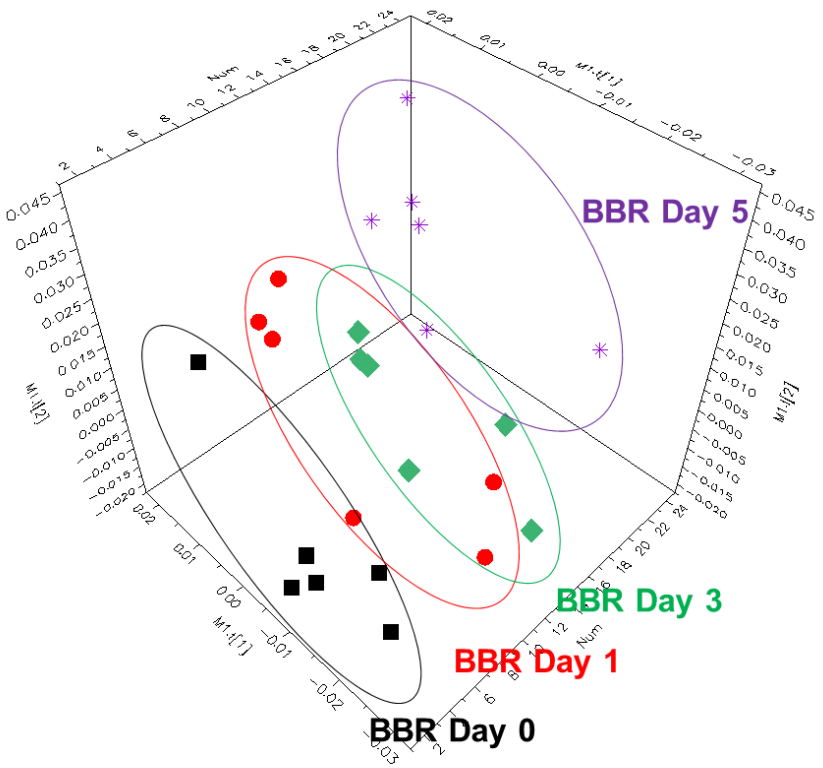

Supplemental Fig. 3 3D PCA scores plot obtained from ^{1}H NMR data from urine after 0 day (■), 1 day (●), 3 days (◆), and 5 days (*) BBR treatment.

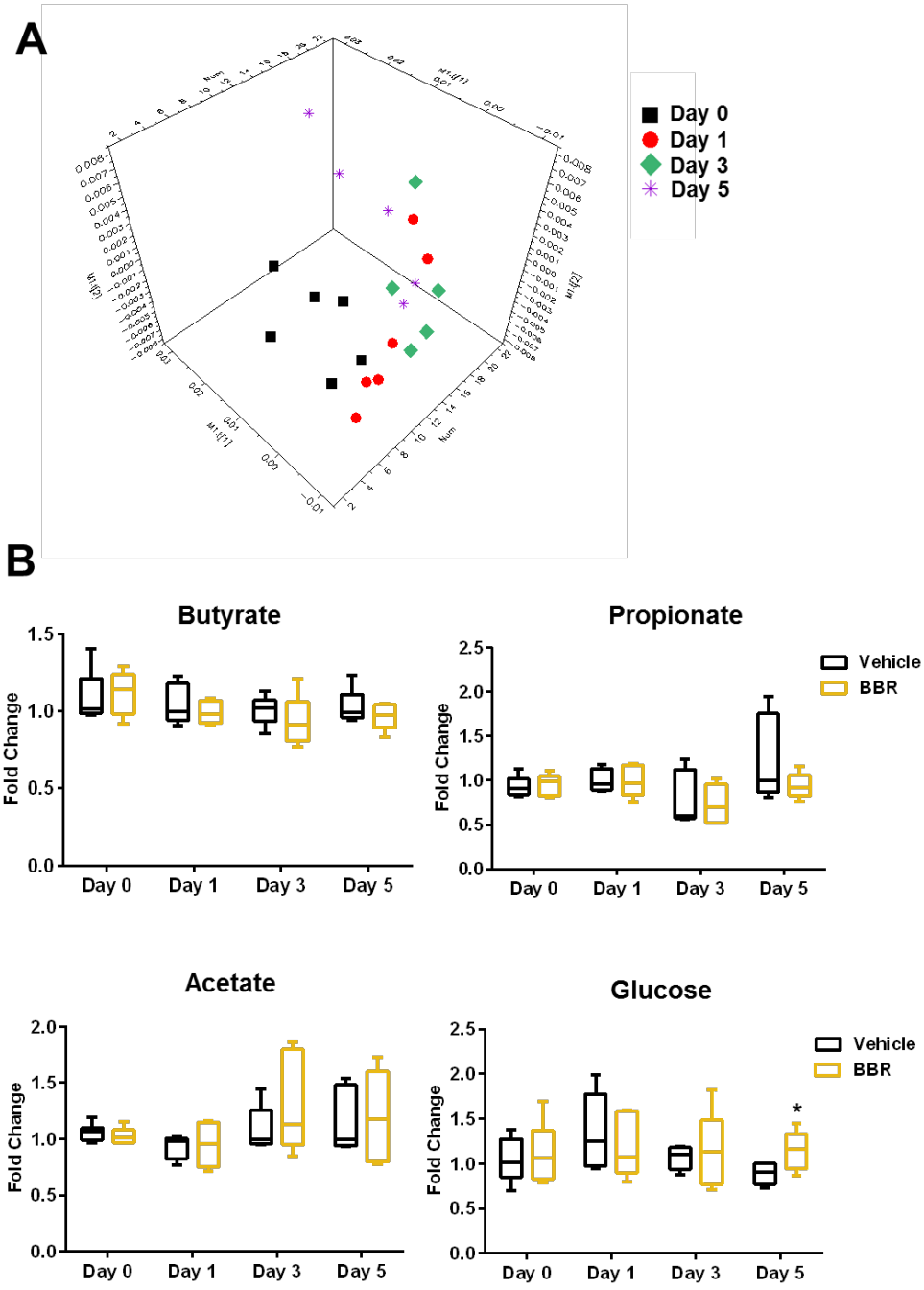

Supplemental Fig. 4 (A) 3D PCA scores plot obtained from ^{1}H NMR data from feces after 0 day (■), 1 day (●), 3 days (◆), and 5 days (*) BBR treatment. (B) Relative abundance of feces metabolites measured by ^{1}H NMR data from mice after 0 day, 1 day, 3 days, and 5 days BBR treatment. Values are the median and interquartile ranges of n = 6 per group.

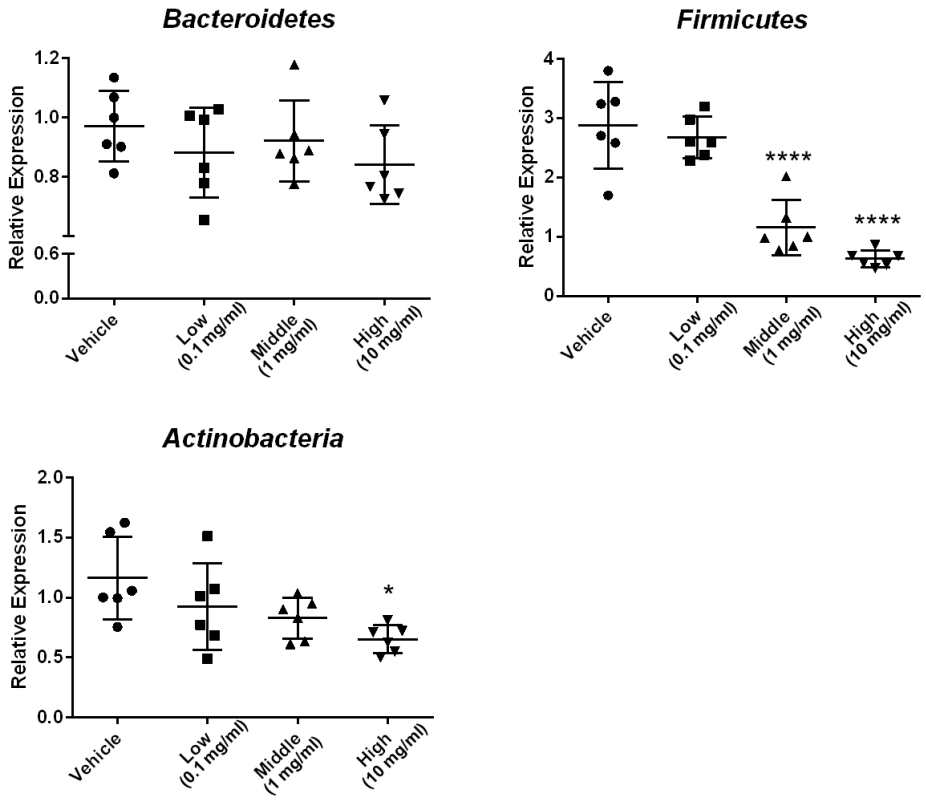

Supplemental Fig. 5 qPCR analysis of bacteria including *Firmicutes*, *Bacteroidetes*, and *Actinobacteria* from cecal bacteria with vehicle or three doses BBR treatment. Values are the mean ± SD of n = 6 per group. * $p < 0.05$, **** $p < 0.0001$

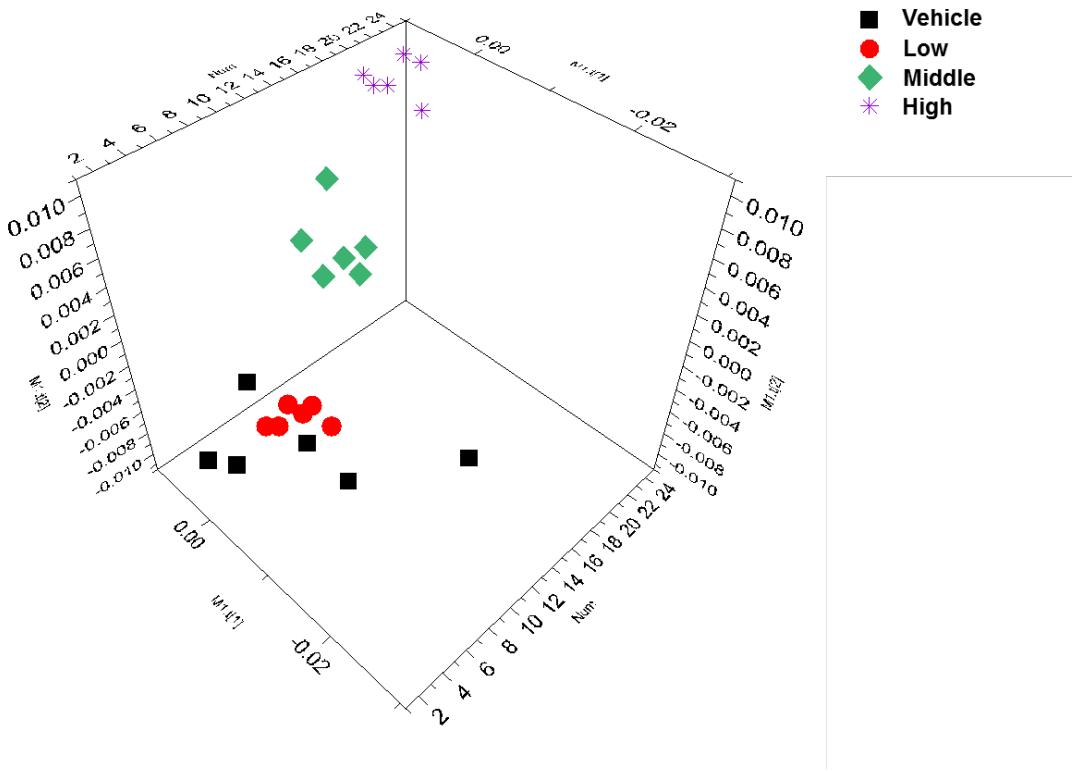

Supplemental Fig. 6 3D PCA scores plot obtained from ^{1}H NMR data from cecal bacteria treated with vehicle (■), low dose BBR (●), middle dose BBR (♦), and high dose BBR (*).